Extending the USGS National Seismic Hazard Maps and ShakeMaps to probabilistic building damage and risk maps

N. Luco & E. Karaca
United States Geological Survey (USGS), Golden, Colorado, USA

(Published in the Proceedings of the 10th Int'l Conf. on Applications of Statistics and Probability in Civil Engineering – 2007)

ABSTRACT: By combining probabilistic hazard curves from the USGS National Seismic Hazard Mapping Project with building fragility curves that we have derived from, in part, FEMA's HAZUS-MH earthquake model for loss estimation, we have prepared preliminary maps of the seismic risk to structures hypothetically located at grid points across the conterminous U.S. In their primary form, the risk maps show the mean annual frequencies of exceeding different structural damage states (none, slight, moderate, extensive, and complete) for each of thirty-six different generic building types (e.g. wood light frame or high-rise steel frame) designed to different code levels (high-, moderate-, low-, and pre-code). Along the same lines, we combine the derived building fragility curves with USGS ShakeMaps of the best estimates of and uncertainties in the ground motions generated by, as an example, the 1994 Northridge earthquake. The result is a map of post-earthquake (but pre-reconnaissance) damage-state probabilities for each of the generic building types and code levels.

1 MOTIVATION

In order for potential losses from earthquakes to be cost-effectively mitigated, whether through improved building codes, retrofit of existing structures, insurance, or emergency response planning, the likelihood of damage and losses (i.e., the seismic risk) must be assessed. The risk depends not only on the location of the structure but also on its type and the level of damage (or loss) of concern.

As a step towards evaluating the seismic risk, the United States Geological Survey (USGS) National Seismic Hazard Maps report the ground motion spectral acceleration values (e.g. at vibration periods of 0.2 and 1.0 seconds) corresponding to various probability of exceedance levels (e.g. 2% and 10% in 50 years). Examples of these maps, from http://earthquake.usgs.gov/research/hazmaps/, are provided in Figure 1. Although they provide the ground motion hazard information needed to compute the risk of damage to structures, the hazard maps themselves do not directly convey this information. As explained below, the computation of risk involves hazard information at multiple probability of exceedance levels, and in some cases at multiple spectral acceleration vibration periods; as mentioned above, it also explicitly depends on the type of structure and the level of damage of concern.

For an individual observed or scenario earthquake, the USGS ShakeMaps (http://earthquake.usgs.gov/eqcenter/shakemap/) report best estimates of ground motion and, as of recently, uncertainties in the ground motions generated by an observed or scenario earthquake. While these data probabilistically describe the ground motions for an individual earthquake, they do not extend this information to fully probabilistic descriptions of the damage to structures. It is the latter that is more directly relevant to post-earthquake emergency response and/or planning.

The HAZUS-MH earthquake model for loss estimation from the U.S. Federal Emergency Management Agency (FEMA) (http://www.fema.gov/plan/prevent/hazus/) can be used to estimate expected (or average) annualized losses or expected losses for scenario earthquakes, but it does not provide *full probability distributions* of annual or scenario losses resulting from damage to structures. Often it is more than the expected losses that are of concern. For example, larger potential losses that are less likely but of high impact can influence decisions regarding building code implementations, retrofits, insurance, and emergency response. Hence, it is full probability distributions of annual losses (for risk maps) or scenario losses (for damage maps) that is the ultimate goal of the work described in this paper.

2 OBJECTIVES

For each grid point on the USGS National Seismic Hazard Maps and each of the thirty-six different

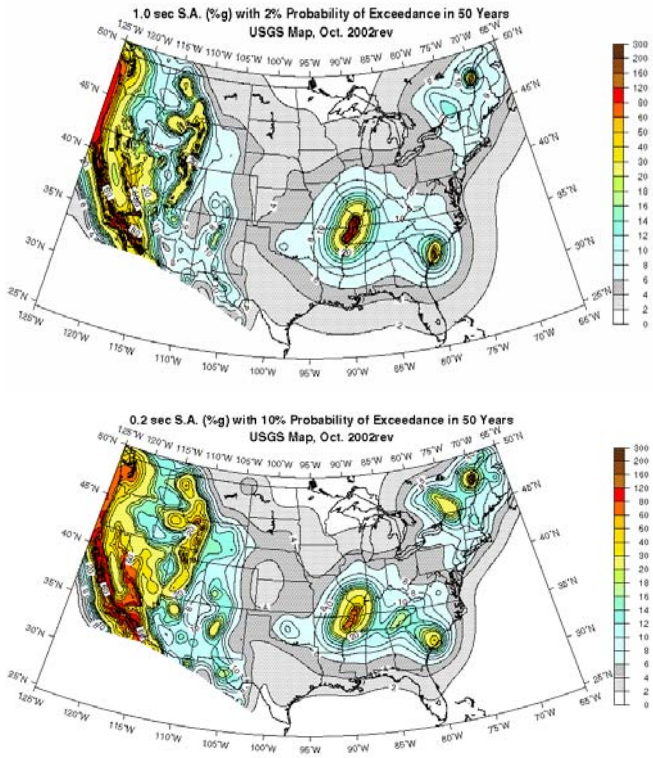

Figure 1. Example USGS National Seismic Hazard Maps.

generic building types (see Table 1) and four different design code levels (high-, moderate-, low-, and pre-code) considered in HAZUS-MH, we combine a seismic hazard curve with building fragility curves for five different structural damage states (none, slight, moderate, extensive, complete) to compute probabilistic "risk maps" that display the mean annual frequency (MAF) of exceeding each damage state. Recall that a seismic hazard curve generally provides the MAFs of exceeding various ground motion spectral acceleration (*SA*) values, and a building fragility curve typically provides the conditional probabilities of exceeding a specified damage state for various *SA* values. The building fragility curves we have developed for this exercise are described in Section 4. Like probabilistic seismic hazard maps, the resulting risk maps consider all potential earthquakes that could affect each location on the grid, and account for their relative frequencies.

Along the same lines, we also combine our building fragility curves with USGS ShakeMaps of the best estimates of and uncertainties in the ground motions generated by the 1994 Northridge earthquake, as an example. The result is a "damage map" of damage-state probabilities (pre-reconnaissance) for each of the generic building types and code levels at each grid point on the ShakeMaps for an observed or scenario earthquake. Note that these damage-state maps reflect the uncertainty in the actual ground motion *SA* values for the earthquake, which (in the case of an observed earthquake) are lowest near ground motion recording stations and higher elsewhere.

Table 1. Building types from HAZUS®MH Technical Manual.

Table 3.1: Building Structure (Model Building) Types

No.	Label	Description	Height			
			Range		Typical	
			Name	Stories	Stories	Feet
1	W1	Wood, Light Frame (≤ 5,000 sq. ft.)		1 - 2	1	14
2	W2	Wood, Commercial and Industrial (> 5,000 sq. ft.)		All	2	24
3	S1L	Steel Moment Frame	Low-Rise	1 - 3	2	24
4	S1M		Mid-Rise	4 - 7	5	60
5	S1H		High-Rise	8+	13	156
6	S2L	Steel Braced Frame	Low-Rise	1 - 3	2	24
7	S2M		Mid-Rise	4 - 7	5	60
8	S2H		High-Rise	8+	13	156
9	S3	Steel Light Frame		All	1	15
10	S4L	Steel Frame with Cast-in-Place Concrete Shear Walls	Low-Rise	1 - 3	2	24
11	S4M		Mid-Rise	4 - 7	5	60
12	S4H		High-Rise	8+	13	156
13	S5L	Steel Frame with Unreinforced Masonry Infill Walls	Low-Rise	1 - 3	2	24
14	S5M		Mid-Rise	4 - 7	5	60
15	S5H		High-Rise	8+	13	156
16	C1L	Concrete Moment Frame	Low-Rise	1 - 3	2	20
17	C1M		Mid-Rise	4 - 7	5	50
18	C1H		High-Rise	8+	12	120
19	C2L	Concrete Shear Walls	Low-Rise	1 - 3	2	20
20	C2M		Mid-Rise	4 - 7	5	50
21	C2H		High-Rise	8+	12	120
22	C3L	Concrete Frame with Unreinforced Masonry Infill Walls	Low-Rise	1 - 3	2	20
23	C3M		Mid-Rise	4 - 7	5	50
24	C3H		High-Rise	8+	12	120
25	PC1	Precast Concrete Tilt-Up Walls		All	1	15
26	PC2L	Precast Concrete Frames with Concrete Shear Walls	Low-Rise	1 - 3	2	20
27	PC2M		Mid-Rise	4 - 7	5	50
28	PC2H		High-Rise	8+	12	120
29	RM1L	Reinforced Masonry Bearing Walls with Wood or Metal Deck Diaphragms	Low-Rise	1-3	2	20
30	RM2M		Mid-Rise	4+	5	50
31	RM2L	Reinforced Masonry Bearing Walls with Precast Concrete Diaphragms	Low-Rise	1 - 3	2	20
32	RM2M		Mid-Rise	4 - 7	5	50
33	RM2H		High-Rise	8+	12	120
34	URML	Unreinforced Masonry Bearing Walls	Low-Rise	1 - 2	1	15
35	URM M		Mid-Rise	3+	3	35
36	MH	Mobile Homes		All	1	10

3 APPROACH

The risk and damage maps are both computed via applications of the theorem of total probability that combine seismic hazard curves and Shakemaps, respectively, with building fragility curves. The details of these combinations are presented below.

3.1 *Risk Maps*

As expressed in Equation 1, the risk maps are computed via integration of the product of (i) the absolute value of the differential of a seismic hazard curve at each grid point and (ii) each of the HAZUS-based but "revamped" building fragility curves that we have developed for this purpose (Karaca and Luco, 2007).

$$\lambda[DS > ds] = \int_{sa} P[DS > ds \mid SA = sa] \; |\, \mathrm{d}\lambda[SA > sa] \,| \qquad (1)$$

In Equation 1, $\lambda[SA>sa]$ denotes the mean annual frequency (MAF) of exceeding a spectral acceleration (*SA*) of *sa*, i.e. a seismic hazard curve like those shown in Figure 2, $P[DS>ds|SA=sa]$ is the conditional probability of exceeding the damage state *ds* given an *SA* of *sa*, i.e. a building fragility curve like those shown in Figure 3; and $\lambda[DS>ds]$ is the resulting MAF of exceeding the damage state *ds*, as shown in Figure 4.

Figure 2. Example USGS seismic hazard curves.

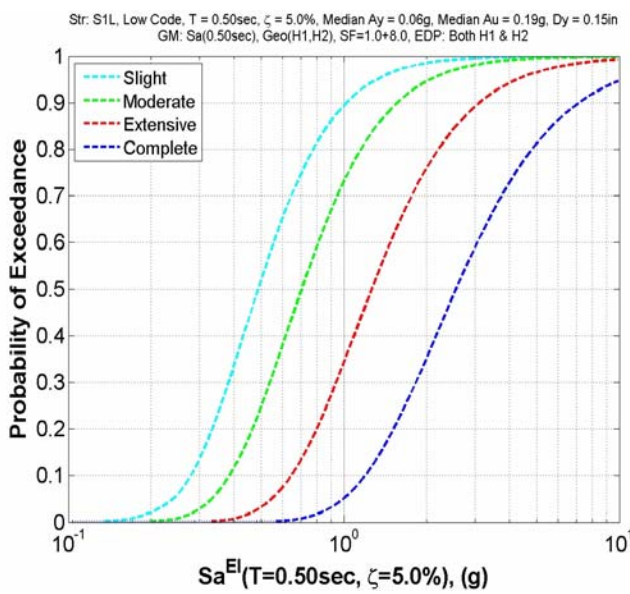

Figure 3. Example structural fragility curves for a generic steel moment frame building (denoted S1L in HAZUS) designed to low code level.

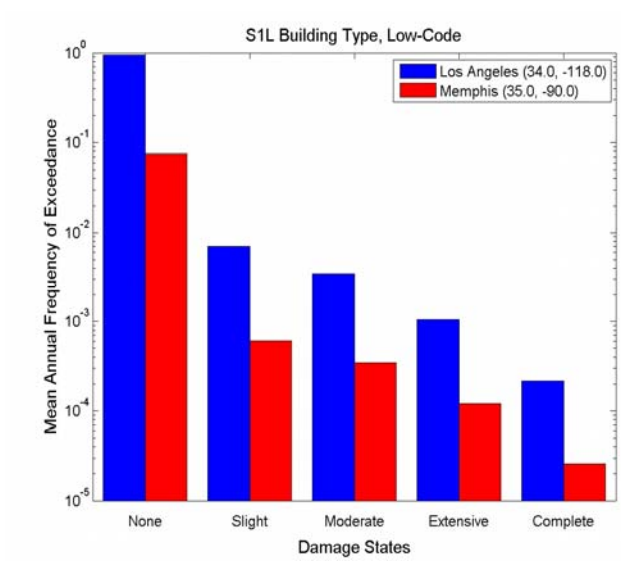

Figure 4. Example risk results computed by combining, via Equation 1, the seismic hazard curves in Figure 2 with the building fragility curves in Figure 3.

3.2 *Damage Maps*

The approach we use to compute probabilistic scenario damage maps based on ShakeMaps, which provide the best estimate of the ground motion *SA* and its uncertainty at each grid point, is analogous to that used for the risk maps, i.e. …

$$P[DS > ds] = \int_{sa} P[DS > ds \mid SA = sa]\; f_{SA}(sa)\, \mathrm{d}sa \quad (2)$$

where $f_{SA}(sa)$ is the probability density function of *SA*, e.g. assuming a lognormal probability distribution. Examples of this integration are provided in Section 6. Note that $f_{SA}(sa)$ can be thought of as a (differenced) hazard curve with reduced uncertainties relative to $\mathrm{d}\lambda[SA>sa]$ due to knowledge of the magnitude, location, and occurrence of the scenario earthquake.

4 BUILDING FRAGILITY CURVES

Since HAZUS does not provide building fragility curves that are functions of the scalar (see the Future Work section of this paper for a comment on the use of vector ground motion intensity measures) elastic spectral acceleration parameters used for the USGS National Seismic Hazard Maps or ShakeMaps, we have developed them using the (i) building capacity curves and associated structural properties and (ii) building fragility curves in terms of inelastic spectral displacement that are defined in HAZUS. We relate elastic spectral acceleration to inelastic spectral displacement via inelastic time-history analysis, in lieu of the Capacity Spectrum Method (e.g. ATC-40) used in HAZUS.

Each of the fragility curves we have developed reflects (i) uncertainties in the building capacity (or "pushover") curve, (ii) variabilities in the building response across different ground motion waveforms with the same *SA* value, and (iii) variabilities in the observed damage state for a given level of building response. The first and third of these uncertainties/variabilities are extracted from HAZUS. We quantify the second, waveform-to-waveform variability in building response by conducting inelastic time-history analysis of a single-degree-of-freedom model of each generic building type subjected to ground motions from the Pacific Earthquake Engineering Research (PEER) Next Generation Attenuation (NGA) Strong Motion Database (http://peer.berkeley.edu/nga/). The results are fragility curves that include the major sources of uncertainty/variability and are in terms of consistent *SA* parameters for combination with the USGS seismic hazard curves and ShakeMaps.

As described more comprehensively in (Karaca & Luco 2007), our step-by-step approach to developing the building fragility curves is as follows:

(1) Define a single-degree-of-freedom (SDOF) oscillator for each generic building type (listed in Table 1) using the vibration periods and backbone curves defined by Table 5.5, and Table 5.7 of the HAZUS Technical Manual, respectively, as well as the damping ratios extracted from HAZUS data files. See the top left panel of Figure 5 for an example backbone curve.

(2) Subject each SDOF oscillator to a large number of ground motion time histories, in this case all those in the PEER Center NGA Strong Motion Database with earthquake moment magnitude larger than 5.0 and closest source-to-site distance between 10km and 80km. For each of these inelastic time history analyses of the SDOF oscillator, the yield and ultimate strengths of the oscillator are randomly and independently generated from a lognormal probability distribution with median from the defined backbone curve and a logarithmic (natural log) standard deviation of 0.25 (0.35 for the pre-code design level). The second and third panels from the top on the left hand side of Figure 5 illustrate one of the inelastic time history analyses, which were performed using a MATLAB function that we developed for the elliptical backbone defined in HAZUS (and Step 1 above) .

(3) Regress the peak oscillator displacement (relative to the ground) resulting from each ground motion, i.e. the inelastic spectral displacement (SD_i), on the corresponding ground motion *SA*. This is done for all of the *SA* vibration periods for which USGS seismic hazard curves and Shakemaps are available, namely 0.0 sec (in which case the *SA* is equivalent to peak ground acceleration), 0.1, 0.2, 0.3, 0.5, 1.0, and 2.0 sec for the hazard curves and 0.0, 0.3, 1.0, and 3.0 sec for the ShakeMaps. Each weighted-least-squares regression analysis results in, after iteration, bilinear relationships between (i) *SA* and the median SD_i and (ii) *SA* and the logarithmic standard deviation of SD_i. An example of the regression results is provided in the second and third panels from the top on the right hand side of Figure 5.

(4) Combine the SD_i on *SA* regression results from Step 3 with the building fragility curves in terms of inelastic spectral displacement that are available from Table 5.9 of the HAZUS Technical Manual (e.g. see the top right panel of Figure 5). These combinations are done using Equation 3 and by assuming that SD_i for a given *SA* is lognormally distributed.

$$P[DS > ds \mid SA = sa] = \int_{sd} P[DS > ds \mid SD_i = sd]\; f_{SD_i|SA}(sd \mid sa)\, \mathrm{d}sd \qquad (3)$$

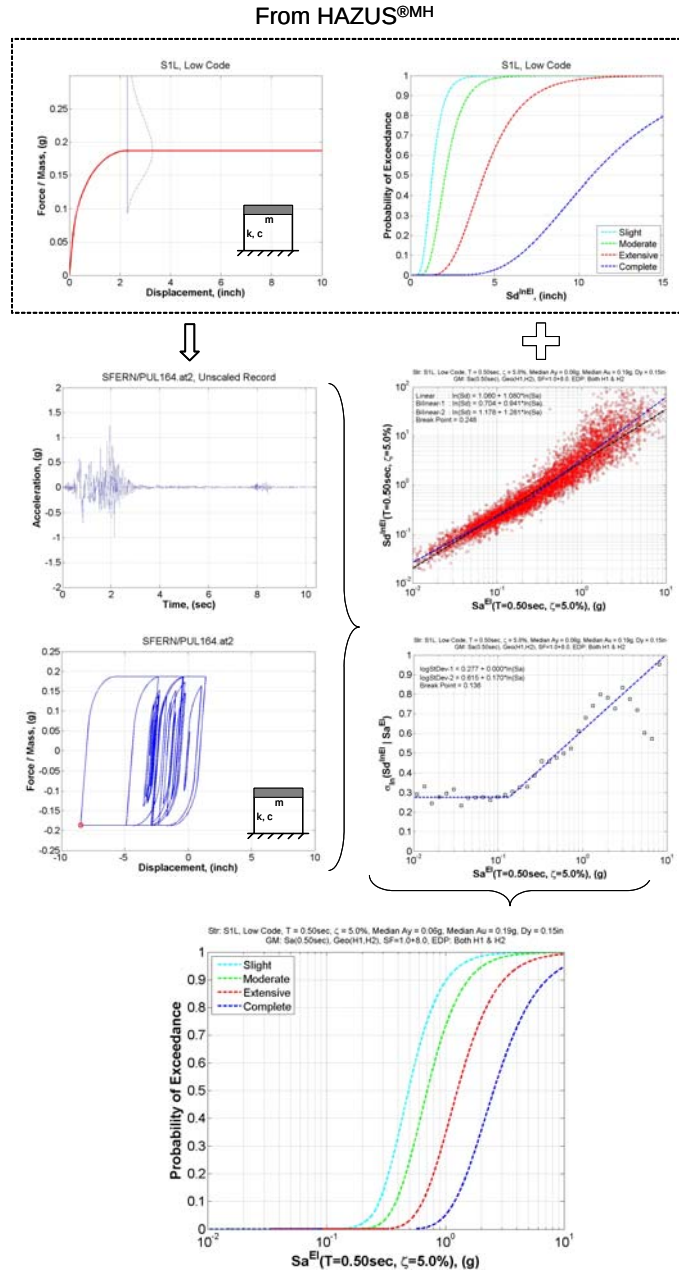

Figure 5. Illustration of the steps taken to develop building fragility curves that are based on HAZUS and can be combined with the USGS National Seismic Hazard Maps or ShakeMaps.

The results of these combinations are the building fragility curves in terms of *SA*. An example is shown in the bottom panel of Figure 5.

4.1 *Comparison with HAZUS for PGA*

Besides its fragility curves in terms of inelastic spectral displacement, the HAZUS Technical Manual also defines building fragility curves in terms of peak ground acceleration (PGA) for all 36 of the generic building types (listed above in Table 1). As a means of validating the building fragility curves that we have derived, we compare our PGA building fragility curves with those defined in Table 5.16 of the HAZUS Technical Manual. In order to make a direct comparison, we have (i) set to zero the variability in *SA* for a given earthquake magnitude and source-to-

site distance that is within the HAZUS fragilities, and (ii) left out (here only) the capacity uncertainty in the derivation of our fragility curves, since this uncertainty is not accounted for in the HAZUS PGA fragilities. For the low-rise steel moment frame building type (S1L), as an example, the results of the comparisons are displayed in Figure 6. Note that there are multiple HAZUS fragility curves for each damage state, one for each of nine magnitude and distance combinations considered in both the Western and Central U.S. Our fragility curves fall within the range of the HAZUS curves. The slopes of our fragility curves are shallower for two reasons: (i) we account for the waveform-to-waveform variability in inelastic spectral displacement for a given value of *SA* (in this case PGA), unlike the HAZUS fragility curves, and (ii) our fragility curves are for a broader range of magnitudes and distances than each of the HAZUS fragility curves. The latter difference will be discussed further in Section 7 (Future Work).

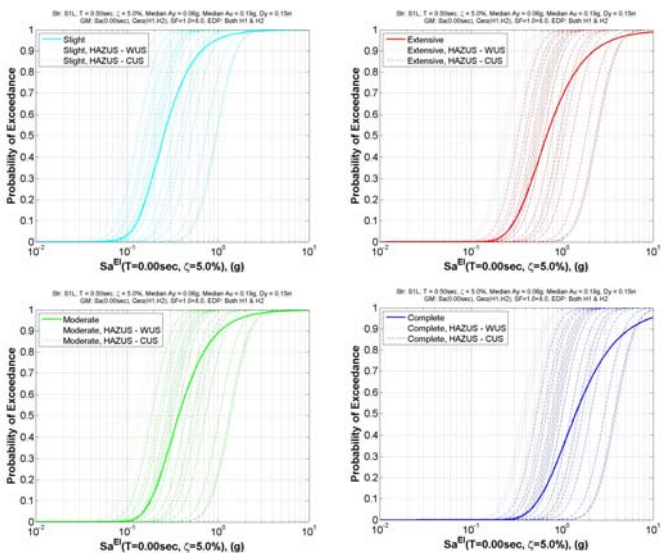

Figure 6. Comparison of our low-rise steel moment frame building (S1L) low-code fragility curves for PGA with the "equivalent PGA" fragility curves defined in HAZUS.

5 EXAMPLE RISK MAPS

For each generic building type (listed in Table 1), seismic design level (high-, moderate-, low-, pre-code), and structural damage state (none, slight, moderate, extensive, complete), we have created seismic risk maps that illustrate the mean annual frequency (MAF) of exceeding the selected damage state, i.e. $\lambda[DS>ds]$. Recall that the corresponding probability of exceeding the damage state at least once in a specified period of time can be found by assuming a Poisson probability distribution of damage state exceedances in time, applying the following equation:

$$P[DS > ds \text{ in } t \text{ years}] = 1 - \exp(-\lambda[DS > ds] \cdot t) \quad (4)$$

Each of the risk maps is generated by evaluating the "risk integral" given in Equation 1 at all of the grid points in the conterminous U.S. for which seismic hazard curves are available from the USGS (from http://earthquake.usgs.gov/research/hazmaps/products_data/2002/hazcurve.php).

Example risk maps for the low-rise steel moment frame building type (S1L), low-code design level, and slight and extensive damage states are shown in Figure 7. Note that the differences between the MAFs of exceedance in Southern California (SoCal) versus the New Madrid Seismic Zone (NMSZ) are different for the slight and extensive damage states.

Low-Rise Steel Moment-Frame Building, Low-Code

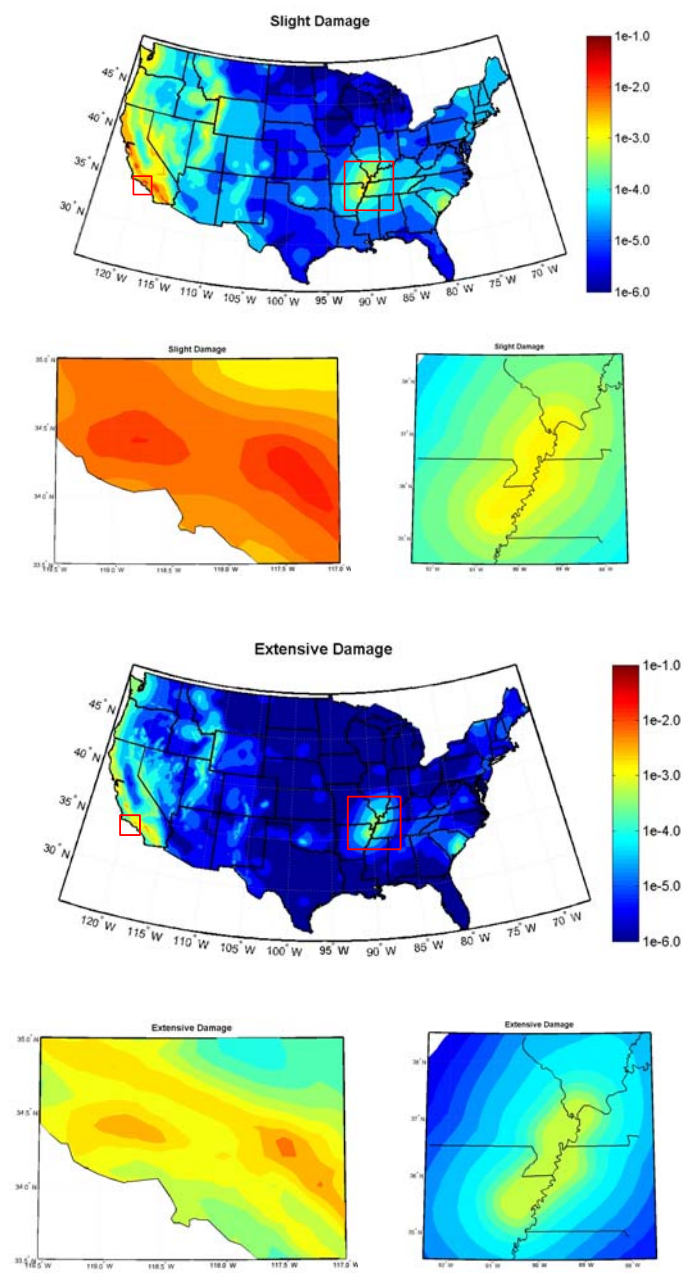

Figure 7. Risk maps illustrating the mean annual of frequency of exceeding slight or extensive damage for a generic low-rise steel moment frame building designed to a low code level.

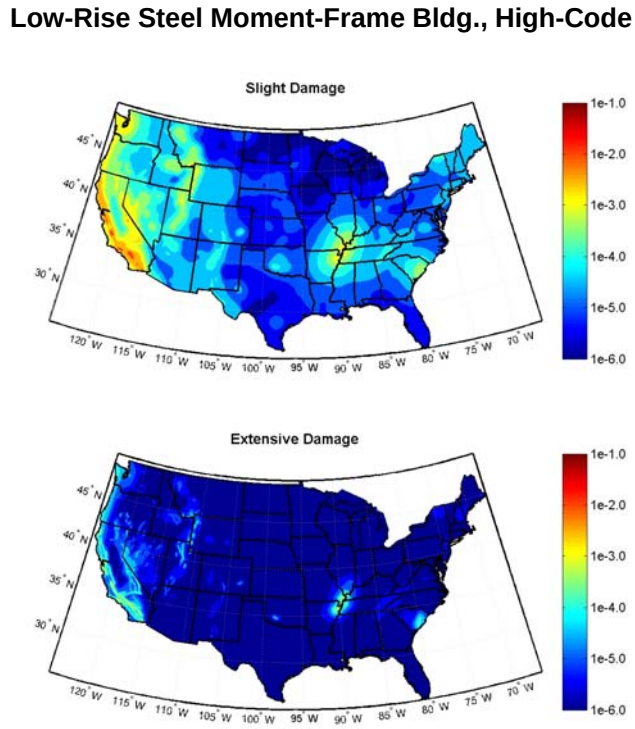

Figure 8. Risk maps illustrating the mean annual of frequency of exceeding slight or extensive damage for a generic low-rise steel moment frame building designed to a *high* code level.

This is because the shapes of the seismic hazard curves in the two regions are significantly different, as illustrated back in Figure 2. Whereas the probabilities of exceeding the relatively large ground motions that contribute most to the extensive damage state are about the same, the probabilities of exceeding the lower ground motions that dominant the slight damage state are lower in the NMSZ relative to SoCal. Furthermore, from a comparison of Figures 7 and 8, note how the high code design level (still for the S1L building type) reduces, relative to the low code design level, the MAFs of exceeding extensive damage more so than those for slight damage. These sorts of insights that affect mitigation decisions cannot be gleaned from seismic hazard maps alone (e.g. Figure 1).

6 EXAMPLE DAMAGE MAPS

In parallel with the risk maps described above, we have generated probabilistic scenario damage maps by evaluating Equation 2 for every grid point on the USGS ShakeMaps for, as an example, the 1994 Northridge Earthquake. The ShakeMap best estimates of and uncertainties in the 1.0-second ground motion *SA* values are illustrated in Figure 9, and the corresponding building fragility curves for the S1L building type are presented in Figure 10. Note that a period of 1.0 seconds is used here for the *SA* in lieu of the 0.5 second period of the S1L building type, since ShakeMaps are not available for the latter period. In fact, 1.0-second *SA* was also used as the ground motion parameter in generating the risk maps in Figures 7-8, for reasons touched upon below in Section 7.

As shown in Figure 10, the building fragility curves combined with the Shakemaps (to create the damage maps) are slightly different than those used with the seismic hazard curves (to create the risk maps in Figures 7-8). This is because the ShakeMaps are in terms of the maximum *SA* across the two horizontal components of ground motion, whereas the USGS seismic hazard curves are (effectively) in terms of the geometric mean *SA* across the two components. As a result, we have developed two parallel sets of building fragility curves in terms of the two ground motion parameters.

The damage map resulting from the combination (via Equation 2) of the ShakeMaps in Figure 9 and the building fragility curves in Figure 10 (for a low-code S1L building) is presented in the top panel of Figure 11. Also shown in Figure 11 are the corresponding damage maps for a generic light-frame wood building (W1) and low-rise unreinforced masonry building (URML), all for a low code design level. The reported probabilities of exceeding slight

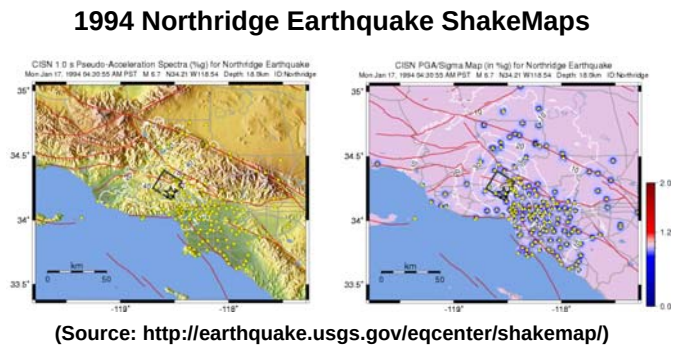

Figure 9. 1994 Northridge Earthquake ShakeMaps for the best estimate of (left panel) and the uncertainty in (right panel) the 1.0-second spectral acceleration. The uncertainty map gives the ratio of the PGA uncertainty to the attenuation relation uncertainty, which is approximately 0.6 in this case; this ratio is assumed to be similar for 1.0-second spectral acceleration.

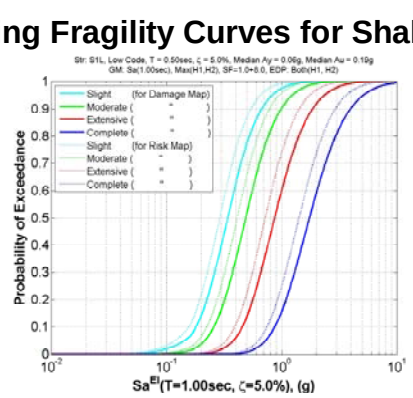

Figure 10. Comparison of our fragility curves for coupling with the USGS National Seismic Hazard Maps versus ShakeMaps, all for a generic low-rise steel moment frame building (S1L) designed to a low-code level.

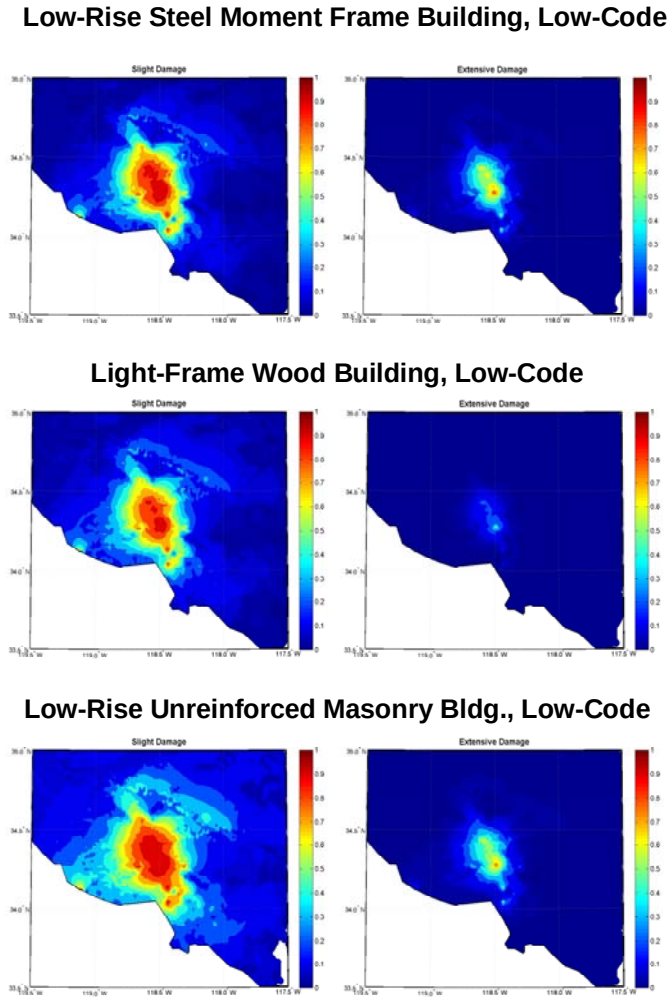

Figure 11. Example damage maps illustrating the probability of exceeding slight and extensive damage for (a) a generic low-rise steel moment frame building, (b) a generic light-frame wood building, and (c) a generic low-rise unreinforced masonry building, all designed to a low code level.

damage indicate that the likelihood of slight or more damage is largest for URML building and smallest for W1 buildings, as one might expect; the likelihood of exceeding slight damage to S1L buildings is comparable to that for the W1 buildings. The likelihood of exceeding *extensive* S1L damage, however, is comparable to that for the URML building type, while the likelihood of exceeding extensive W1 damage remains the lowest. Results like these can be useful in, for example, directing emergency response efforts.

7 FUTURE WORK

Though widely used, elastic spectral acceleration at or near the fundamental building period (*SA*) has been demonstrated to be an "insufficient" ground motion intensity measure with respect to inelastic displacement response (e.g. Luco & Cornell, 2007). As a result, the building fragility curves we have developed are not always independent of the earthquake magnitudes (*M*) and source-to-site distances (*R*) of the ground motion waveforms used, as

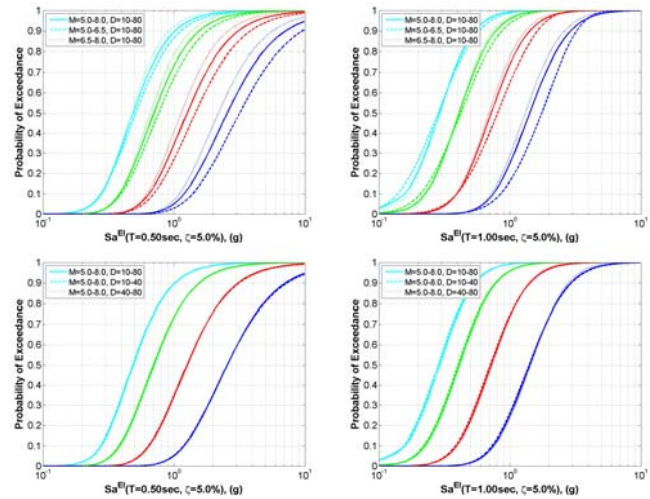

Figure 12. Using building fragility curves for a generic low-rise steel moment frame building designed to a low-code level, an illustration of the dependence on magnitude (top row) and distance (bottom row) when using 0.5-second (left column) versus 1.0-second (right column) spectral acceleration. Recall that the four different colors correspond to the slight, moderate, extensive, and complete damage states.

demonstrated in the figures below. To remove this dependence, we plan to develop building fragility surfaces that are functions of both *SA* and ground motion epsilon (e.g. Baker & Cornell, 2005) or *M* and *R*. In either case, the seismic hazard information in terms of the vector ground motion intensity measure that is needed to compute the risk maps will incorporate (e.g., *ala* Bazzurro & Cornell, 2002) USGS deaggregations for each geographic location. Alternatively, we may develop building fragility curves that are a function of *SA* alone, but that vary with geographic location and the associated deaggregation information (e.g. *ala* Shome & Cornell, 1999). In the meantime, for each building fragility curve we have selected the *SA* period that minimizes the dependence on *M* and *R*, e.g. 1.0-second SA instead of 0.5-second SA for the S1L building type, as demonstrated in Figure 12.

8 CONCLUSIONS

The preliminary risk maps and damage maps described in this paper extend the USGS National Seismic Hazard Maps and ShakeMaps and provide probabilistic structural damage information. Note that the HAZUS default values of direct economic losses corresponding to each of the five structural damage states (enumerated above) are 0%, 2%, 10%, 50%, and 100% of the building's replacement cost, respectively. In this way, the risk maps also provide information about the probability distributions of losses (including, but beyond, average annual losses) for different types of buildings designed to different code levels at different geographic locations in the U.S. An extension to direct economic

losses that takes into account the variability in loss for a given damage state is planned for future work.

The same steps taken to develop the structural fragility curves described in this paper have recently been carried out to develop the corresponding non-structural drift- and acceleration-sensitive fragility curves. By expressing the three sets of fragility curves in terms of the loss percentages mentioned above, and by making assumptions about the correlations between the three types of damage, we have developed probabilistic relations between spectral acceleration and total (structural plus nonstructural) loss percentages. When monetary losses rather than physical structural or nonstructural damage is the primary concern, such loss functions provided the requisite link between seismic hazard and risk.

9 REFERENCES

FEMA (2003). “HAZUS-MH Technical Manual,” Federal Emergency Management Agency, Washington, D.C.

Karaca E and Luco N (2007). “Development of Seismic-Hazard-Compatible Building Fragility Functions: Application to HAZUS Building Types,” In preparation.

Frankel AD, Petersen MD, Mueller CS, Haller KM, Wheeler RL, Leyendecker EV, Wesson RL, Harmsen SC, Cramer CH, Perkins DM, and Rukstales KS (2002). “Documentation for the 2002 Update of the National Seismic Hazard Maps,” U.S Geological Survey Open File Report 02-420.

Wald DJ, Worden BC, Quitoriano V, and Pankow KL (2006). “ShakeMap Manual,” U.S. Geological Survey Techniques and Methods 12-A1.

California Seismic Safety Commission (1996). “Seismic evaluation and retrofit of concrete buildings,” ATC-40, Redwood City, CA.

Luco N and Cornell CA (2007). “Structure-Specific Scalar Intensity Measures for Near-Source and Ordinary Earthquake Ground Motions,” Earthquake Spectra, Volume 23, Issue 2.

Baker JW and Cornell CA (2005). “A Vector-Valued Ground Motion Intensity Measure consisting of Spectral Acceleration and Epsilon,” Earthquake Engineering & Structural Dynamics, 34(10):1193-1217.

Bazzurro P and Cornell CA (2002). “Vector-Valued Probabilistic Seismic Hazard Analysis (VPSHA),” Proceedings of the 7th U.S. National Conference on Earthquake Engineering, Paper No. 61, Boston, Massachusetts.

Shome N and Cornell CA (1999). "Probabilistic Seismic Demand Analysis of Nonlinear Structures," Reliability of Marine Structures Program Report No. RMS-35, Department of Civil and Environmental Engineering, Stanford University, California.